ARTICLE

Vector Correlations and Product Rotational Alignments of Reactions Ca+RBr→CaBr+R (R=CH_3, C_2H_5 and n-C_3H_7)

Jian-jun Ma, Shu-lin Cong*, Zhi-hong Zhang, Yan-qiu Wang

Department of Physics, Dalian University of Technology, Dalian 116024, China

(Dated: Received on February 3, 2005; Accepted on April 30, 2005)

The quasiclassical trajectory method is used to study the vector correlations of the reactions Ca+RBr (R=CH_3, C_2H_5 and n-C_3H_7Br) and the rotational alignment of product CaBr. The product rotational alignment parameters at different collision energies and the vector correlations between the reagent and product are numerically calculated. The vector correlations are described by using the angle distribution functions $P(\theta_r)$, $P(\phi_r)$, $P(\theta_r, \phi_r)$ and the polarization-dependent differential cross sections (PDDCSs). The peak values of $P(\theta_r)$ of the product CaBr from Ca+CH_3Br are larger than those from Ca+C_2H_5Br and Ca+n-C_3H_7Br. The peak of $P(\theta_r)$ at $\phi_r = 3\pi/2$ is apparently stronger than that at $\phi_r = \pi/2$ for the three reactions Ca+RBr. The calculation results show that the rotational angular momentum of the product CaBr is not only aligned, but also oriented along the direction which is perpendicular to the scattering plane. The product CaBr molecules are strongly scattered forward. The orientation and alignment of the product angular momentum will affect the scattering direction of the product molecules to varying degrees.

Key words: Quasiclassical trajectory, Vector correlation, Orientation and alignment

I. INTRODUCTION

It is important to study the vector properties of reagent and product in order to fully understand the molecular reaction dynamics [1-11]. The analysis of vector properties reveals rich molecular reaction dynamical information. The most important vector correlation for the reaction A+BC→AB+C is the $\mathbf{k}-\mathbf{k}'-\mathbf{j}'$ correlation (where $\mathbf{k}$ and $\mathbf{k}'$ respectively denote the relative velocity vectors of reagent and product, and $\mathbf{j}'$ represents the rotational angular momentum of the product). The correlations among the three vectors in the center-of-mass (CM) frame can be described by the interesting double and triple vector correlation functions.

Experimentally, there are many techniques to measure the vector correlations between reagent and product. Zare and co-workers [12,13] used the REMPI detection and the core extraction technique to measure the angular momentum alignments of the products HCl and DCl from the reactions Cl+CH_4 and Cl+C_2D_6. Brouard *et al.* utilized the techniques of photon-initiated bimolecular reaction and Doppler resolved laser-induced fluorescence to obtain the desired stereodynamical information from the reactions H+CO_2 and H+N_2O [14,15]. The measurement of product polarization as a function of scattering angle was achieved by using the photoloc method [16,17]. The product rotational alignments in the reactions of alkaline earth atoms with brominated aryl were probed by using the laser-induced chemiluminescence and the polarized laser-induced fluorescence [11,18].

Theoretically, the quasiclassical trajectory, quantum-scattering and wave packet dynamics methods have been employed to describe the vector correlations and the angular momentum polarizations of the reagent and product [19-21]. Hijazi and Polanyi used the quasiclassical trajectory (QCT) method to investigate the effects of different mass combinations on the product angular distributions [20]. Shafer-Ray *et al.* put forward the concept of polarization dependent differential cross-sections (PDDCSs) [22]. Clary and co-workers derived the quantum mechanical expressions for describing stereodynamics of atom-diatom reactions [23,24]. Aoiz and co-workers presented a detailed and quantitative comparison of the quantum mechanical and quasiclassical descriptions of the stereodynamics of elementary chemical reactions [25]. They also described the vector correlation $\mathbf{k}-\mathbf{k}'-\mathbf{j}'$ between the reagent and product in photo-initiated bimolecular reaction [19]. Han and co-workers studied the product rotational polarizations of bimolecular reactions with different reagent mass combinations on attractive, mixed and repulsive potential energy surfaces [7,21,26].

Reactions between alkaline earth metal atoms and halogenated hydrocarbon molecules have been extensively studied. Han and co-workers probed the CaBr($B^2\Sigma^+$) product alignment in the reactions of Ca ($^1P_1$) with C_2H_5Br and n-C_3H_7Br by means of the laser-induced chemiluminescence under single-collision conditions in a beam-gas arrangement [18]. In the present work, we focus on the vector correlations of reactions Ca+RBr (R=CH_3, C_2H_5 and n-C_3H_7) and the rotational alignment of product CaBr.

*Author to whom correspondence should be addressed. E-mail: shlcong@dlut.edu.cn

II. THEORY

A. Vector correlations between reagent and product

The z-axis of the center-of-mass (CM) frame is chosen to be parallel to the reagent relative velocity $\mathbf{k}$, and the y-axis is perpendicular to the xz plane containing $\mathbf{k}$ and $\mathbf{k}'$, as shown in Fig.1. The fully correlated center-of-mass angular distribution is given by [19,22]

$$P(\omega_t,\omega_r)=\sum_{kq}\frac{2k+1}{4\pi}\frac{1}{\sigma}\frac{\mathrm{d}\sigma_{kq}}{\mathrm{d}\omega_t}C_{kq}(\theta_r,\phi_r)^* \qquad (1)$$

where $C_{kq}(\theta_r,\phi_r)=\sqrt{4\pi/(2k+1)}\,Y_{kq}(\theta_r,\phi_r)$ is the modified spherical harmonics. $(1/\sigma)(\mathrm{d}\sigma_{kq}/\mathrm{d}\omega_t)$ denotes a polarization-dependent differential cross section (PDDCS), which is defined as

$$\frac{1}{\sigma}\frac{\mathrm{d}\sigma_{kq}}{\mathrm{d}\omega_t}=\int P(\omega_t,\omega_r)\,C_{kq}(\theta_r,\phi_r)\mathrm{d}\omega_r \qquad (2)$$

where $\mathrm{d}\omega_r=\sin\theta_r\mathrm{d}\theta_r\mathrm{d}\phi_r$. The PDDCS with $q\neq0$ can be written as [19]

$$\begin{aligned}\frac{1}{\sigma}\frac{\mathrm{d}\sigma_{kq\pm}}{\mathrm{d}\omega_t}&=\frac{1}{\sigma}\frac{\mathrm{d}\sigma_{kq}}{\mathrm{d}\omega_t}\pm\frac{1}{\sigma}\frac{\mathrm{d}\sigma_{k-q}}{\mathrm{d}\omega_t}\\&=\sum_{k_1}\frac{2k_1+1}{4\pi}S^{(k_1)}_{kq\pm}C_{k_1-q}(\theta_t,0) \qquad (3)\\S^{(k_1)}_{kq\pm}&=\langle C_{k_1q}(\theta_t,0)C_{kq}(\theta_r,0)\\&\quad\times\left[(-1)^q e^{iq\phi_r}\pm e^{-iq\phi_r}\right]\rangle \qquad (4)\end{aligned}$$

where the angular bracket represents an average over all angles. The PDDCS with $q\neq0$ satisfies the conditions

$$\frac{1}{\sigma}\frac{\mathrm{d}\sigma_{kq+}}{\mathrm{d}\omega_t}=0,\ k\text{ even},\ q\text{ odd or }k\text{ odd},\ q\text{ even} \qquad (5)$$

$$\frac{1}{\sigma}\frac{\mathrm{d}\sigma_{kq-}}{\mathrm{d}\omega_t}=0,\ k\text{ even},\ q\text{ even or }k\text{ odd},\ q\text{ odd} \qquad (6)$$

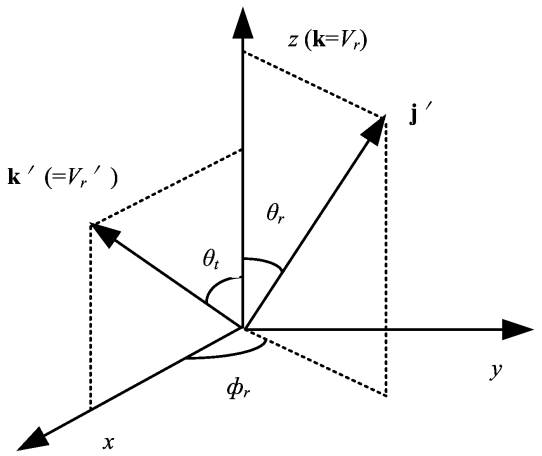

FIG. 1 The center-of mass coordinate system for describing the $\mathbf{k}$, $\mathbf{k}'$ and $\mathbf{j}'$ distribution

The PDDCS with q=0 is given by

$$\begin{aligned}\frac{1}{\sigma}\frac{\mathrm{d}\sigma_{k0}}{\mathrm{d}\omega_t}&=\frac{1}{4\pi}\sum_{k_1}(2k_1+1)\,\langle P_{k_1}(\cos\theta_t)\\&\quad\cdot P_k(\cos\theta_r)\rangle\,P_{k_1}(\cos\theta_t) \qquad (7)\end{aligned}$$

with the condition

$$\frac{1}{\sigma}\frac{\mathrm{d}\sigma_{k0}}{\mathrm{d}\omega_t}=0,\quad k\ \text{ is odd} \qquad (8)$$

In the computation, PDDCSs are expanded up to k_1=7, which is sufficient for good convergence. Many photoinitiated bimolecular reaction experiments are sensitive only to the polarization moments with k=0 and k=2. Hence, four polarization moments ($\mathrm{d}\sigma_{00}/\mathrm{d}\omega_t$, $\mathrm{d}\sigma_{20}/\mathrm{d}\omega_t$, $\mathrm{d}\sigma_{22+}/\mathrm{d}\omega_t$ and $\mathrm{d}\sigma_{21-}/\mathrm{d}\omega_t$) are calculated in our work.

The distribution function $P(\theta_r)$ describing the two-vector correlation ($\mathbf{k}$–$\mathbf{j}'$) can be expanded in a series of Legendre polynomials as

$$\begin{aligned}P(\theta_r)&=\frac{1}{2}\sum_k(2k+1)\,{a_0}^k P_k(\cos\theta_r) \qquad (9)\\a_0^{(k)}&=\int_0^\pi P(\theta_r)P_k(\cos\theta_r)\sin\theta_r\mathrm{d}\theta_r\\&=\langle P_k(\cos\theta_r)\rangle \qquad (10)\end{aligned}$$

The expanding coefficients $a_0^{(k)}$ or $\langle P_k(\cos\theta_r)\rangle$ are called orientation (odd k) and alignment (even k) parameters. In our computation, $P(\theta_r)$ is expanded up to k=18, which shows good convergence.

The dihedral angle distribution function $P(\phi_r)$ describing $\mathbf{k}$–$\mathbf{k}'$–$\mathbf{j}'$ correlation can be expanded as a Fourier series

$$\begin{aligned}P(\phi_r)&=\frac{1}{2\pi}\Bigg(1+\sum_{\text{even }n\geq2}a_n\cos n\phi_r\\&\quad+\sum_{\text{odd }n\geq1}b_n\sin n\phi_r\Bigg) \qquad (11)\\a_n&=2\,\langle\cos n\phi_r\rangle\,,\quad b_n=2\,\langle\sin n\phi_r\rangle \qquad (12)\end{aligned}$$

In the computation, $P(\phi_r)$ is expanded up to n=24, which shows good convergence.

The distribution function $P(\theta_r,\phi_r)$ describing the direction of $\mathbf{j}'$ can be written as

$$\begin{aligned}P(\theta_r,\phi_r)&=\frac{1}{4\pi}\sum_{kq}(2k+1)a_q^{(k)}C_{kq}(\theta_r,\phi_r)^* \qquad (13)\\a_q^{(k)}&=\int C_{kq}(\theta_r,\phi_r)P(\theta_r,\phi_r)\mathrm{d}\omega_r\\&=\langle C_{kq}(\theta_r,\phi_r)\rangle \qquad (14)\end{aligned}$$

The expanding coefficients $a_q^{(k)}$ or $\langle C_{kq}(\theta_r,\phi_r)\rangle$ are the generalized orientation (odd k) and alignment (even k) parameters. When q=0, Eq.(14) reduces to Eq.(10). In the computation, $P(\theta_r,\phi_r)$ is expanded up to k=7, which is sufficient for good convergence.

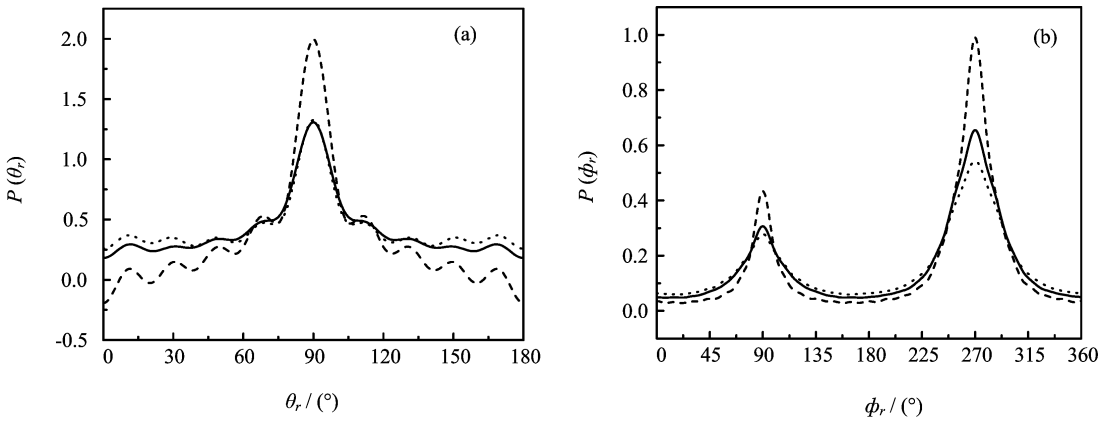

FIG. 2 The vector correlations at the collision energy of 7.54 kJ/mol for the reactions Ca+RBr→CaBr+R (R=CH_3, C_2H_5 and n-C_3H_7). (a) The $P(\theta_r)$ distributions, and (b) the $P(\phi_r)$ distributions. The dash line, solid line and dot line show the reactions Ca+CH_3Br, Ca+C_2H_5Br and Ca+n-C_3H_7Br, respectively.

B. Quasiclassical trajectory calculation

The calculating method of quasiclassical trajectories is the same as Ref.[26-28]. The classical Hamilton's equations are numerically integrated in three dimensions. In the calculation, a batch of 4×10^5 trajectories are run for each of the reactions Ca+RBr (R=CH_3, C_2H_5 and n-C_3H_7). The integration step size is chosen as 0.1 fs. The values of the maximum impact parameter $b_{\max}$ are listed in Table I. The initial atom-molecular separation is chosen to be ρ=15.0 Å. The extended London-Eyring-Polanyi-Sato (LEPS) potential energy surfaces are employed in our calculations [18,21,24]. The parameters of potential energy surfaces for the reactions Ca+RBr→CaBr+R are listed in Table II [18].

III. RESULTS AND DISCUSSION

The rotational alignment parameters $\langle P_2(\cos\theta_r)\rangle$ of the product CaBr from the reactions Ca+RBr (R=CH_3, C_2H_5 and n-C_3H_7) at different collision energies are calculated and the results are shown in Table I.

TABLE I The calculated values of alignment parameters of the product CaBr from three reactions.

Reaction	$E_{\rm col}$/(kJ/mol)	$\langle\cos^2\theta_r\rangle$	$b_{\max}$/Å	$\langle P_2\cos\theta_r\rangle$
Ca+CH_3Br	7.54	0.112	7.9	−0.332
	18.84	0.086	6.8	−0.371
	24.28	0.078	6.5	−0.383
Ca+C_2H_5Br	7.54	0.207	8.5	−0.190
	18.84	0.155	7.0	−0.268
	24.28	0.139	6.8	−0.292
Ca+n-C_3H_7Br	7.54	0.228	8.5	−0.158
	18.84	0.221	7.2	−0.169
	24.28	0.198	6.8	−0.203

$\langle P_2(\cos\theta_r)\rangle$ ranges in value from −0.5 to 1. When $\langle P_2(\cos\theta_r)\rangle$= −0.5 and 1, $\mathbf{j}'$ are perpendicular and parallel to $\mathbf{k}$, respectively. From Table I we find that product rotational alignment parameters are negative for the collision energies used in the computations, which indicates that the angle θ_r between $\mathbf{j}'$ and $\mathbf{k}$ is in the range from 54.736° to 125.264°. For a fixed collision energy, for example, $E_{\rm col}$= 7.54 kJ/mol, the absolute magnitude of $\langle P_2(\cos\theta_r)\rangle$ decreases as the atomic numbers of radical group R increase. For a given reaction, for instance, Ca+CH_3Br, the absolute magnitude of $\langle P_2(\cos\theta_r)\rangle$ increases with the increase of the collision energy. The rotational angular momentum of the product CaBr tends to be perpendicularly polarized with respect to the relative velocity vector $\mathbf{k}$ of reagents. In the case of the collision energy being 7.54 kJ/mol, the experimental values of alignment parameters $\langle P_2(\cos\theta_r)\rangle$ of the product CaBr from the reactions Ca+C_2H_5Br and Ca+n-C_3H_7Br are −0.18±0.02 and −0.14±0.02, respectively [18]. The calculated results shown in Table I are consistent with the experimental ones.

In order to obtain a graphical description of the vector correlations, we plot the angular distribution curves of vector correlation functions $P(\theta_r)$ and $P(\phi_r)$ in Fig.2 (where $P(\theta_r)$ and $P(\phi_r)$ are not normalized). In the computation, the collision energy (i.e., the relative translational energy) is chosen as 7.54 kJ/mol,

TABLE II Parameters used in the LEPS potential energy surface for the reactions Ca+RBr→CaBr+R (R=CH_3, C_2H_5 and n-C_3H_7Br) [18].

Species	D_e/eV	β_i/Å^{-1}	R_0/Å	S_i
CH_3Br	3.073	1.681	1.94	0.992
C_2H_5Br	3.073	1.681	1.94	0.992
n-C_3H_7Br	3.024	1.695	1.94	0.992
CaBr	4.077	0.990	2.57	0.605
CaR	1.950	1.326	2.33	−0.882

which is the value used in the experiment of Ca+RBr reaction [18].

The distribution function $P(\theta_r)$ describes the $\mathbf{k}-\mathbf{j}'$ correlation. It can be seen from Fig.2 (a) that the $P(\theta_r)$ peaks at $\theta_r=\pi/2$ and is symmetric with respect to $\pi/2$. This result shows that the product rotational angular momentum vector is strongly aligned along the direction at right angle to the relative velocity direction. The peak of $P(\theta_r)$ of the product CaBr from Ca+CH_3Br is stronger than those from Ca+C_2H_5Br and Ca+n-C_3H_7Br. The distribution curves of $P(\theta_r)$ from Ca+C_2H_5Br and Ca+n-C_3H_7Br are very much alike in shape.

Figure 2 (b) shows the dihedral angle distributions $P(\phi_r)$ of the product CaBr. The $P(\phi_r)$ are asymmetric with respect to the $\mathbf{k}-\mathbf{k}'$ scattering plane (or about $\phi_r=\pi$). The peaks of $P(\phi_r)$ appear at $\phi_r=\pi/2$ and $3\pi/2$, which show that the angular momentum vector of CaBr is aligned along y-axis of the CM frame. Because the peak at $\phi_r= 3\pi/2$ is apparently stronger than that at $\phi_r=\pi/2$, the angular momentum vector of CaBr is not only aligned, but also oriented along the negative diraction of y-axis. The orientation of the product molecule mainly results from the repulsion between R (CH_3, C_2H_5 and n-C_3H_7) and Br. For Ca+RBr→CaBr+R reaction, the angular momentum $\mathbf{j}'$ of the product CaBr can be expressed as [29-32]

$$\mathbf{j}' = \mathbf{l}\sin^2\beta + \mathbf{j}\cos^2\beta + \mathbf{J}_1\frac{m_{\rm Br}}{m_{\rm CaBr}} \qquad (15)$$

$$\cos^2\beta = \frac{m_{\rm Ca}m_{\rm R}}{(m_{\rm Ca}+m_{\rm Br})(m_{\rm Br}+m_{\rm R})} \qquad (16)$$

$$\mathbf{J}_1 = \sqrt{\mu_{\rm RBr}\Re}(\mathbf{r}_{\rm CaBr}\times\mathbf{r}_{\rm RBr}) \qquad (17)$$

where $\mathbf{l}$ and $\mathbf{j}$ denote the reagent orbital and rotational angular momenta, respectively. $\cos^2\beta$ represents the mass factors, which are 0.053, 0.089 and 0.117 for the reactions Ca+CH_3Br, Ca+C_2H_5Br and Ca+n-C_3H_7Br, respectively. $\mu_{\rm RBr}$ is the reduced mass of the RBr molecule and $\Re$ the repulsive energy between R and Br. $\mathbf{r}_{\rm CaBr}$ and $\mathbf{r}_{\rm RBr}$ are unit vectors that Br points to Ca and R, respectively. During the chemical bond forming and breaking for the Ca+RBr reaction, $\mathbf{l}\sin^2\beta+\mathbf{j}\cos^2\beta$ in Eq.(15) is symmetric with respect to the $\mathbf{k}-\mathbf{k}'$ scattering plane. However, $\mathbf{J}_1 m_{\rm Br}/m_{\rm CaBr}$ tends to a preferred direction because of the effect of the repulsive energy, which causes the orientation of the product CaBr [32].

Figure 3 depicts the angular distributions $P(\theta_r,\phi_r)$ of the product CaBr from the reactions Ca+RBr (R=CH_3, C_2H_5 and n-C_3H_7). The peaks of $P(\theta_r,\phi_r)$ appear at (θ_r,ϕ_r)=($\pi/2$,$\pi/2$) and ($3\pi/2$,$3\pi/2$), which are consistent with the distributions of $P(\theta_r)$ and $P(\phi_r)$.

Figure 4 shows the distributions of four PDDCSs with the angle θ_t between $\mathbf{k}$ and $\mathbf{k}'$ for the reactions Ca+RBr (R=CH_3, C_2H_5 and n-C_3H_7). The three reactions have similar results. The PDDCSs describe the $\mathbf{k}-\mathbf{k}'-\mathbf{j}'$ correlation and the scattering direction of the product molecule. $(2\pi/\sigma)(d\sigma_{00}/d\omega_t)$ is proportional to the differential cross section. It only describes the $\mathbf{k}-\mathbf{k}'$ correlation or the scattering direction of the product molecule and is not associated with the orientation and alignment of the product angular momentum $\mathbf{j}'$. It can be seen from the distribution of $(2\pi/\sigma)(d\sigma_{00}/d\omega_t)$ that the product molecules are strongly scattered forward and weakly scattered sideways and backward. The distribution of $(2\pi/\sigma)(d\sigma_{20}/d\omega_t)$ indicates that the product molecules are scattered forward. $(2\pi/\sigma)(d\sigma_{20}/d\omega_t)$ is related to $P_2(\cos\theta_r)$. The distribution of $(2\pi/\sigma)(d\sigma_{20}/d\omega_t)$ displays a trend that is opposite to that of $(2\pi/\sigma)(d\sigma_{00}/d\omega_t)$ because the expected values $\langle P_2(\cos\theta_r)\rangle$ are negative (see Table I). We can see that the alignment of the prod-

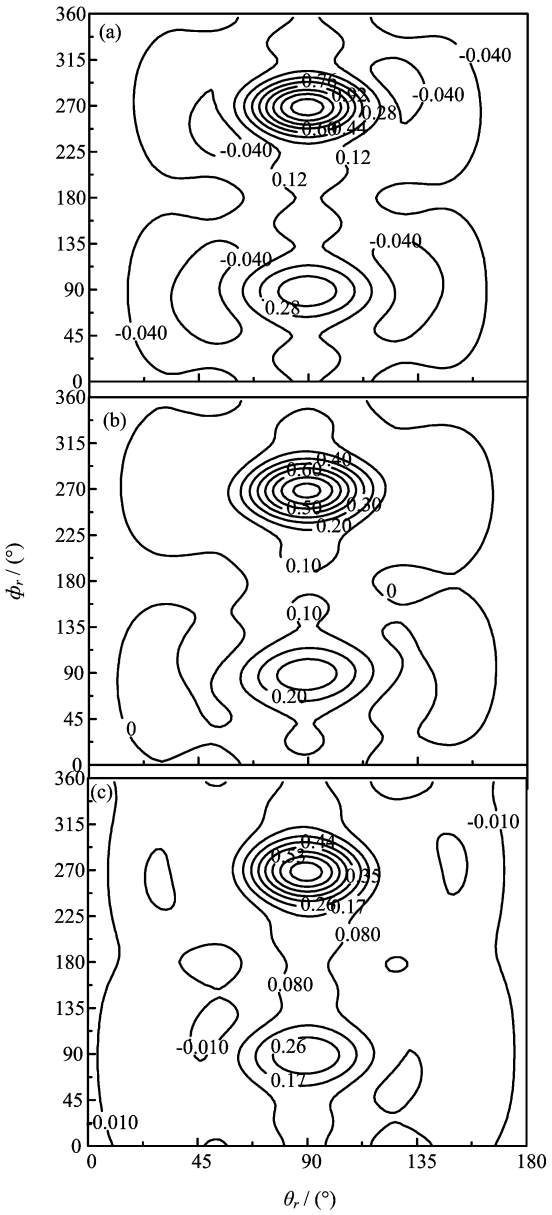

FIG. 3 Polar plots of $P(\theta_r,\phi_r)$ distributions at the collision energy of 7.54 kJ/mol for the three reactions: (a) Ca+CH_3Br, (b) Ca+C_2H_5Br and (c) Ca+n-C_3H_7Br.

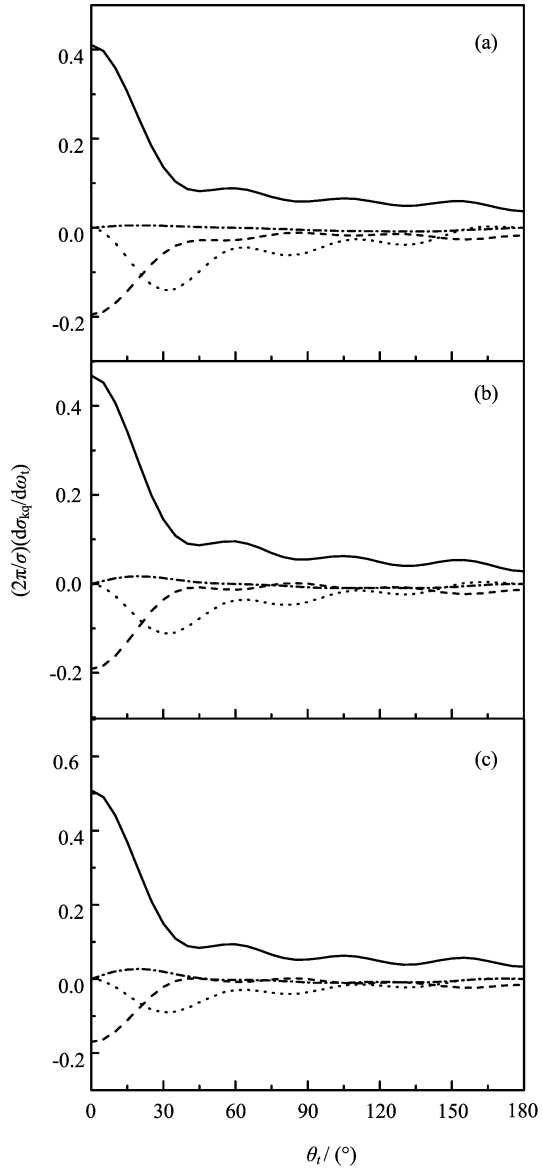

FIG. 4 The vector correlations at the collision energy of 7.54 kJ/mol for (a) Ca+CH_3Br, (b) Ca+C_2H_5Br and (c) Ca+n-C_3H_7Br. The solid line, dash line, dot line and dash dot line show $(2\pi/\sigma)(d\sigma_{00}/d\omega_t)$, $(2\pi/\sigma)(d\sigma_{20}/d\omega_t)$, $(2\pi/\sigma)(d\sigma_{22+}/d\omega_t)$ and $(2\pi/\sigma)(d\sigma_{21-}/d\omega_t)$, respectively. All PDDCSs are depicted in arbitrary unit.

uct angular momentum $\mathbf{j}'$ has a great influence on the distributions of $(2\pi/\sigma)(d\sigma_{20}/d\omega_t)$. The PDDCS with $q\neq0$ at the scattering angles away from the extreme forward and backward directions provide information on the ϕ_r dihedral angle distribution and are nonzero at scattering angles away from θ_r=0 and π, which indicates that the $P(\theta_r,\phi_r)$ distribution is not isotropic for sideways scattering products. The variations of the PDDCSs with k=2 reflect the changes of the rotational polarization with the scattering angles. The value of $(2\pi/\sigma)(d\sigma_{21-}/d\omega_t)$ is close to zero at all the angles θ_t. In other words, it is obviously isotropic and almost independent of the scattering angle θ_t. This results from the fact that $(2\pi/\sigma)(d\sigma_{21-}/d\omega_t)$ is related to $\sin2\theta_r\cos\phi_r$ or $P(\theta_r,\phi_r)$. From the distribution of $P(\theta_r,\phi_r)$, the strong peaks appear at (θ_r,ϕ_r)=(π/2,π/2) and (3π/2,3π/2). As a result, $\sin2\theta_r\cos\phi_r$ or $(2\pi/\sigma)(d\sigma_{21-}/d\omega_t)$ is close to zero. The $(2\pi/\sigma)(d\sigma_{22+}/d\omega_t)$ is relative to $\langle\sin^2\theta_r\cos2\phi_rY_{k_12}(\theta_t,0)\rangle$. From the distribution of $(2\pi/\sigma)(d\sigma_{22+}/d\omega_t)$, the product molecules are scattered sideways. The strongest scattering peak appears at θ_t=π/6. At the extremes of forward and backward scattering (θ_t=0 and π), the expected value of $Y_{k_12}(\theta_t,0)$ is equal to zero, which leads to $(2\pi/\sigma)(d\sigma_{22+}/d\omega_t)$=0. Further, at θ_t=0 and π, the $\mathbf{k}-\mathbf{k}'$ scattering plane can not be determined and the values of PDDCSs with $q\neq0$ must be zero.

Finally, in order to study the effect of collision energy on dihedral angle distribution $P(\phi_r)$, we depict the distribution of $P(\phi_r)$ at different collision energies for the reaction Ca+n-C_3H_7Br→CaBr+n-C_3H_7, as shown in Fig.5. The other two reactions have similar results. The peak values of $P(\phi_r)$ change with the collision energy, but the positions of peaks are invariable for different collision energies. When the collision energy increases, the peak value of $P(\phi_r)$ at ϕ_r=π/2 decreases and that at ϕ_r=3π/2 increases. Moreover, the area under distribution curve of $P(\phi_r)$ dose not change with the collision energy because $\int P(\phi_r)\,d\phi_r$= constant.

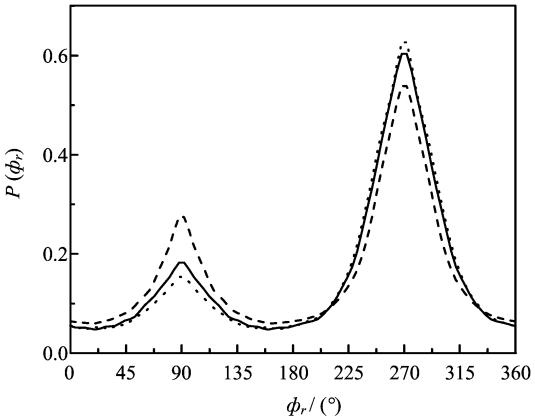

FIG. 5 The dihedral angular distributions $P(\phi_r)$ with respect to the $\mathbf{k}-\mathbf{k}'$ plane for reaction Ca+n-C_3H_7Br→CaBr+n-C_3H_7 at different collision energies. The dash line, solid line and dot line show the calculated results at the collision energies 7.54, 18.84 and 24.28 kJ/mol, respectively.

IV. CONCLUSIONS

We have employed the quasiclassical trajectory method to study the vector correlations between the product and reagent for the reactions Ca+RBr (R=CH_3, C_2H_5 and n-C_3H_7). We have calculated the product rotational alignment parameters at differ-

ent collision energies and plotted the angle distribution curves of $P(\theta_r)$, $P(\phi_r)$, $P(\theta_r, \phi_r)$ and PDDCSs. The peak value of $P(\theta_r)$ of the product CaBr from Ca+CH_3Br is larger than those from Ca+C_2H_5Br and Ca+n-C_3H_7Br. The peak of $P(\phi_r)$ at ϕ_r=$3\pi/2$ is apparently stronger than that at ϕ_r=$\pi/2$. We can conclude from the angular distribution of $P(\theta_r)$, $P(\phi_r)$ and $P(\theta_r, \phi_r)$ that the rotational angular momentum of the product CaBr is not only aligned, but also oriented along the y-axis that is perpendicular to the $\mathbf{k}-\mathbf{k}'$ scattering plane. The PDDCSs describe the $\mathbf{k}-\mathbf{k}'-\mathbf{j}'$ correlation and the scattering direction of the product CaBr. From the distributions of PDDCSs we arrive at the conclusion that the product CaBr molecules are strongly scattered forward for the reactions Ca+RBr. The orientation and alignment of the product angular momentum will affect the scattering direction of the product molecule to varying degrees.

V. ACKNOWLEDGMENT

This work is supported by the National Natural Science Foundation of China (No.10374012).

[1] J. D. Barnwell, J. G. Loeser and D. R. Herschbach, J. Phys. Chem. **87**, 2781 (1983).
[2] B. Soep and R. Vetter, J. Phys. Chem. **99**, 13569 (1995).
[3] X. Zhang, T. X. Xie, M. Y. Zhao and K. L. Han, Chin. J. Chem. Phys. **15**, 169 (2002).
[4] M. D. Chen, B. Y. Tang, K. L. Han and N. Q. Lou, Chin. J. Chem. Phys. **15**, 247 (2002).
[5] S. L. Cong, Y. M. Li, H. M. Yin, J. L. Sun and K. L. Han, Chin. J. Chem. Phys. **15**, 198 (2002).
[6] J. Y. Liu, W. H. Fan, K. L. Han, D. L. Xu and N. Q. Lou, Chin. J. Chem. Phys. **16**, 161 (2003).
[7] M. L. Wang, K. L. Han, J. P. Zhan, V. W. K. Wu, G. Z. He and N. Q. Lou, Chem. Phys. Lett. **278**, 307 (1997).
[8] M. L. Wang, K. L. Han and G. Z. He, J. Chem. Phys. **109**, 5446 (1998).
[9] K. L. Han, G. Z. He and N. Q. Lou, J. Chem. Phys. **96**, 7865 (1992).
[10] K. L. Han, G. Z. He and N. Q. Lou, Chem. Phys. Lett. **193**, 165 (1992).
[11] J. P. Zhan, H. P. Yang, K. L. Han, W. Q. Deng, G. Z. He and N. Q. Lou, J. Phys. Chem. A **101**, 7486 (1997).
[12] A. J. Orr-Ewing, W. R. Simpson, S. A. Kandel, T. P. Rakitzis and R. N. Zare, J. Chem. Phys. **106**, 5961 (1997).
[13] T. P. Rakitzis, S. A. Kandel, T. Lev-On and R. N. Zare, J. Chem. Phys. **107**, 9392 (1997).
[14] M. Brouard, S. D. Gatenby, D. M. Joseph and C. Vallance, J. Chem. Phys. **113**, 3162 (2000).
[15] M. Brouard, I. Burak, D. W. Hughes, K. S. Kalogerakis, J. P. Simons and V. Stavros, J. Chem. Phys. **113**, 3173 (2000)
[16] H. Loesch, J. Phys. Chem. **101**, 7461 (1997).
[17] H. L. Kim, M. A. Wickramaaratchi, X. Zheng and G. E. Hall, J. Chem. Phys. **101**, 2033 (1994).
[18] K. L. Han, L. Zhang, D. L. Xu, G. Z. He and N. Q. Lou, J. Phys. Chem. A **105**, 2956 (2001).
[19] F. J. Aoiz, M. Brouard and P. A. Enriquez, J. Chem. Phys. **105**, 4964 (1996).
[20] N. H. Hijazi and H. C. Polanyi, J. Chem. Phys. **63**, 2249 (1975).
[21] K. L. Han, G. Z. He and N. Q. Lou, J. Chem. Phys. **105**, 8699 (1996).
[22] N. E. Shafer-Ray, A. J. Orr-Ewing and R. N. Zare, J. Phys. Chem. **99**, 7591 (1995).
[23] M. P. De Miranda and D. C. Clary, J. Chem. Phys. **106**, 4509 (1997).
[24] M. P. De Miranda, D. C. Clary, J. F. Castillo and D. E. Manolopoulos, J. Chem. Phys. **108**, 3142 (1998).
[25] M. P. De Miranda, F. J. Aoiz, L. Bañares and V. Sáez Rábanos, J. Chem. Phys. **111**, 5368 (1999).
[26] M. L. Wang, K. L. Han, G. Z. He and N. Q. Lou, J. Phys. Chem. A **102**, 10204 (1998).
[27] M. D. Chen, M. L. Wang, K. L. Han and S. L. Ding, Chem. Phys. Lett. **301**, 303 (1999).
[28] L. Zhang, M. D. Chen, M. L. Wang and K. L. Han, J. Chem. Phys. **112**, 3701 (2000).
[29] K. L. Han, G. Z. He and N. Q. Lou, Chin. J. Chem. Phys. **2**, 323 (1989).
[30] R. J. Li, K. L. Han, F. E. Li, R. C. Lu, G. Z. He and N. Q. Lou, Chin. J. Chem. Phys. **6**, 1 (1993).
[31] R. J. Li, K. L. Han, R. C. Lu, G. Z. He and N. Q. Lou, Chem. Phys. Lett. **220**, 281 (1994).
[32] M. D. Chen, K. L. Han and N. Q. Lou, Chem. Phys. Lett. **357**, 483 (2002).